ANALELE ŞTIINTIFICE ALE UNIVERSITĂŢII „ALEXANDRU IOAN CUZA" din IAŞI
Tom LXIII, nr.1, s. IIc, Geografie 2018
ISSN 1223-5334 (printed version)

SCIENTIFIC ANNALS OF „ALEXANDRU IOAN CUZA" UNIVERSITY OF IAŞI
Volume LXIII, no.1, s. II c, Geography series 2018
(online version) 2284-6379 eISSN

HYDROLOGIC RESPONSE TO LAND USE CHANGE AND CLIMATE VARIABILITY IN AN UNGAUGED BASIN, NORTH-WESTERN HIMALAYA, INDIA

Narender VERMA[1], Pratik DASH[2]

[1]Department of Geography, Banarah Hindu University, India
[2]Centre for the Study of Regional Development, Jawaharlal Nehru University, New Delhi, India
e-mail: nverma1972@gmail.com, pratik.bidyut@gmail.com

Abstract: Hydrological models are overwhelmingly used for gauged basins to simulate variations in water balance components from environmental changes. Unavailability of hydro-meteorological data restricts model applications for ungauged basins, though the remotely sensed data can be used as a substitute for a solution. In the present study, we used Soil and Water Assessment Tool (SWAT) to investigate the impacts of land use land cover (LULC) change and climate variability on hydrological regime of an ungauged river basin (Sirsa river) in north-western Himalaya, India for the period 1983–2008. The model was calibrated and validated (2004–2008) using MODIS actual evapotranspiration data (MOD16A2) with high monthly concordance (R2=0.81). The results showed that remotely sensed evapotranspiration data could be used as a proxy of gauge discharge data to calibrate the physically-based model. The substantial increase in built-up area (6.5%) and cropland (9.8%) over forest cover and barren land caused a corresponding increase in average annual surface runoff (12%) and a decrease in lateral flow (6.7%) from base level LULC of 1989 to 2009. The climate variability alone was found significant to reduce average annual streamflow (26.5%) in monsoon season (wet), baseflow (6.5%) and lateral flow (4.6%) in the dry period. While considering combined impacts, the changes in average annual surface runoff and streamflow are dominantly influenced by climate variability; while lateral flow, baseflow and percolation are largely controlled by LULC change. As the water resources of the study area are expected to be adversely effected in the near future, this study will effectively benefit stakeholders and administrators for the management of water resources. Besides, to improve our knowledge for better understanding of the hydrologic consequence of LULC change, this study will help to enhance the scope hydrologic modeling for data-poor regions.

Keywords: *LULC change; climate variability; ungauged basin; SWAT; MODIS evapotranspiration data*

I. INTRODUCTION

Land use land cover (LULC) and climate are the most crucial parameters controlling hydrological processes. Globally, river basin hydrological systems are increasingly getting affected by LULC and climate changes induced by human activity. As a result, water related problems e.g., flood, water scarcity, water pollution, and sedimentation are mainly manifested; mostly in developing countries like India where rapid and unplanned development is severely affecting land ecosystems.

LULC change and climate change may lead annual and seasonal changes in hydrological processes through altering canopy cover and evapotranspiration (Mao and Cherkauer, 2009; Beck et al., 2013), infiltration capacity and soil water content (Zhang and Schilling, 2006), streamflow components (Wu and Johnston, 2007; Zhang et al., 2007, Tan et al., 2015), groundwater recharge (Eshtawi et al., 2015), flood frequency (Gu et al., 2011; Sanyal et al., 2014) etc. While conversion of forest cover to agriculture can lead to an increase in peak runoff (Peña-Arancibia et al., 2012; Babar and Ramesh, 2015), forest regeneration may increase actual evaporation with insignificant change in streamflow (Beck et al., 2013). Urbanization and deforestation can alter water movement from sub-surface flow to overland flow, resulting in high stream discharge and high sediment loss; and low local water availability in dry period (Costa et al., 2003). As LULC is likely expected to change in future, it will assert significant influence on regional and global hydrological cycle (Anav et al., 2010; Deng et al., 2015).

Combining geographical information system (GIS) with remote sensing data various distributed hydrological models are fruitfully applied to investigate the impact of LULC change and climate variability on hydrological response at various spatial and temporal scales. Previous research studied hydrologic response to: (i) LULC change (Nie et al., 2011; Baker and Miller, 2013; Li et al., 2013; Tran and O'Neill, 2013); (ii) climate change (Githui et al., 2009; Wilson and Weng, 2011; Jha and Gassman, 2014); and (iii) simultaneous effect of LULC change and climate change (Wang et al., 2009; Wilson and Weng, 2011; Zhao et al., 2015). These studies account: (i) assessment of past changes using historical records; and (ii) changes in future hydrological behavior based on scenario generated from climatic model and the relationship of past changes.

Combined effect of LULC change and climate change on hydrological processes are quite complex. A clear understanding of these effects separately on hydrological regimes is essential to project future hydrologic conditions (Wilson and Weng, 2011) and water resources management. Concomitantly, the degree of influence of each LULC types on hydrology is also important to understand (Nie et al., 2011; Li et al., 2013; Yan et al., 2013). Most of the previous studies are mainly confined to gauged basins in various countries across the world, including USA (Tran and O'Neill, 2013; Jha and Gassman, 2014), Australia (Peña-Arancibia et al., 2012; Beck et al., 2013), Europe (Eckhardt and Ulbrich, 2003; Guan et al., 2015), Africa (Mango et al., 2011; Baker and Miller, 2013), China (Li et al., 2013; Yan et al., 2013). Hydrological modeling for developing countries, where catchment information and hydro-meteorological data are poorly available, is very challenging but essential.

Regionalization is a very popular method for hydrological modeling of ungauged catchments, wherein calibrated model parameters are transferred from gauged (donor) to ungauged (target) catchment based on spatial proximity or physical similarity (Parajka et al., 2005; Götzinger and Bárdossy, 2007; Samuel et al., 2011). But, uncertainty in the simulation may arise either due to equifinality problems from optimisation with a limited number of gauge points (Beven and Freer, 2001), or parameter transfer through regionalization approach (Sellami et al. 2014). Moreover, what to do when donor (gauged) basin is not available? Satellite-based remote sensing data can be used to overcome this problem with a broad spatial and temporal coverage (Lakshmi, 2004). Remote sensing data have been used to derive various hydrological variables including: (i) evapotranspiration estimation (Immerzeel and Droogers, 2008; Jhorar et al., 2011; Githui et al., 2012); (ii) infiltration estimation (Frappart et al., 2008); and (iii) streamflow estimation (Zhang et al., 2004; Callow and Boggs, 2013).

Remote sensing data derived vegetation cover and leaf area index (Chen et al., 2005; Immerzeel and Droogers, 2008), soil moisture (Campo et al., 2006), snow cover (Stehr et al., 2009), and meteorological data (Andersen et al., 2002) have been used as inputs in various distributed and semi-distributed models for calibration and hydrological assessment. Few of the above mentioned studies derived actual evapotranspiration (ETa) from MODIS normalized differenced vegetation index (NDVI) and leaf area index (LAI) using surface energy balance algorithm for land (SEBAL) algorithm, and used it as observed ETa to calibrate SWAT model for estimating water balance. But, calculation of long term ETa from MODIS data using SEBAL method is quite complex and labour intensive. Ready-made ETa data product of MODIS (MOD16A2) for the globe with 1 km resolution (Mu et al., 2007) is very useful to calibrate hydrological model easily for ungauged basins.

The integration of remote sensing data derived hydrological variables with hydrological models to calibrate and assess the impact of LULC change and climate variability on hydrology in data-sparse river basin of developing countries is not well established. Coupled with three periods LULC data (1989, 1999 and 2009) and climate data (1983–2008), the Soil and Water Assessment Tool (SWAT) model was used in this study for hydrologic simulation of Sirsa river basin in north-western Himalaya, India. Three specific objectives of this paper are: (i) calibration of SWAT model parameters with MODIS ET data for ungauged river basin; (ii) assessment of individual impact of LULC change and climate variability on average annual and seasonal water balance components; and (iii) estimation of combined effect of LULC change and climate variability on major hydrological components.

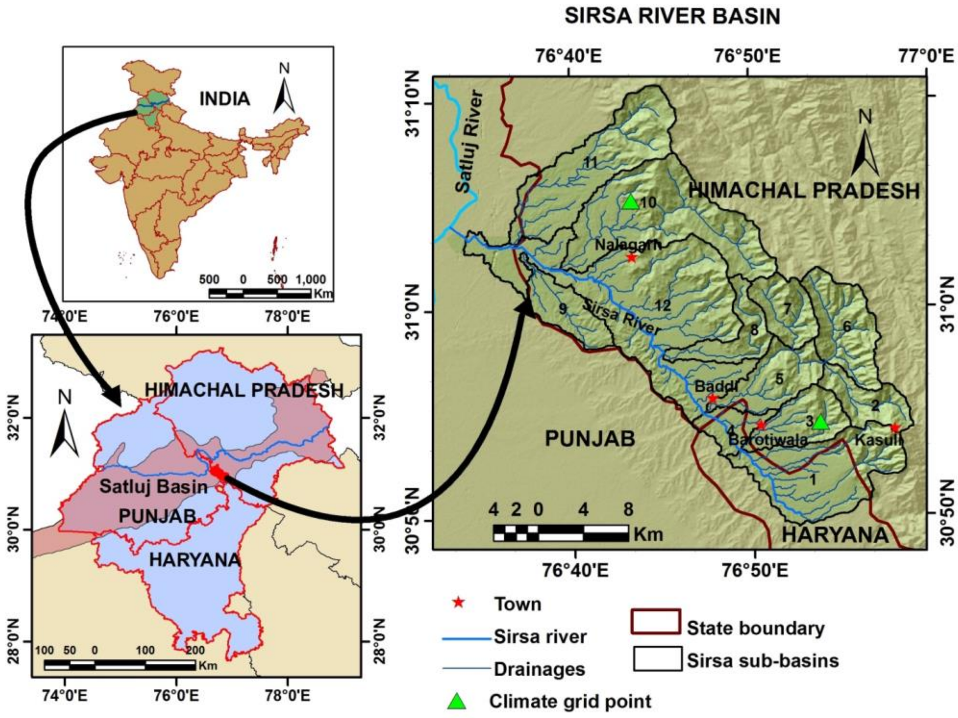

Fig. 1 Location map of Sirsa river basin, including towns, climate grid points and sub-basins. The numbers in Sirsa river basin map indicate corresponding sub-basin ID (#).

II. MATERIALS AND METHODS

II.1 Study site

Sirsa river basin, a downstream tributary of Satluj River, is located at the fringe of north-western Himalaya covering 680 km2 geographical area in between 30°49′22″ to 31°11′00″ N and 76°32′48″ to 76°59′22″ E. (Figure 1). Topographically, the basin is sandwiched between the sub-Himalayan ranges in the north and north-east, and Siwaliks in the south and southwest giving it a typical ridge and valley topographic character (Dash et al., 2014). Elevation of the basin varies between 250 and 1900 m with an average of 615 m, almost half of which is characterized by an intermontane valley (Nalagarh valley). Two types of soil i.e. loamy and loamy-skeletal found the basin (Figure 2). The soil in the intermontane region is moderately porous, and moderate to high in thickness; while in sub-Himalayan mountains soil is less thick and highly efficient for runoff generation. Meteorologically, the basin is located in sub-tropical monsoon climate with a mean annual temperature of 23.5 oC and a mean annual precipitation of 900 mm. Most of the rainfall (about 80%) is received during monsoon period (June-September), maximally in July.

Forest, cropland, barren land and built-up area are the major LULC types noticed in the basin. About half of the basin area is covered with forests, mostly short to medium in height. Agriculture is extensively practiced both in the low-lying intermontane valleys and upland regions along the mountain slopes in the form of terrace farming. Major crops of the basin are maize, wheat, and paddy cultivated during Kharif and Rabi seasons. Massive industrialization in the past two decades has dramatically altered the land use pattern in the Sirsa river basin. Baddi-Barotiwala-Nalagarh area located within the study area is the biggest industrial hub in the Solan district, Himachal Pradesh, India. Since last two decades, rapid industrialization has caused significant growth in population. As per the census of India (2011), the population of Nalagarh and Baddi town increased by 13.40% and 32.34%, respectively during 2001–2011.

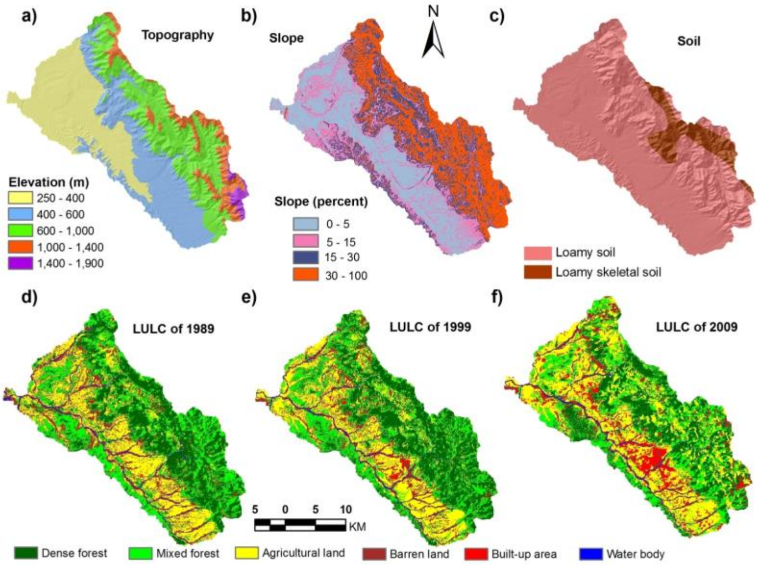

Fig. 2 Basin characteristics used in SWAT model including a) elevation, (b) slope, (c) soil types, and land use map of (d) 1989, (e) 1999 and (f) 2009.

II.2. Materials

The Advanced Spaceborne Thermal Emission and Reflection Radiometer (ASTER) Global Digital Elevation Model (GDEM) of 1 arc-second (~30 m) is used for topographical input (hereafter DEM). The input data layer of soil (1:125,000), including soil types and properties, was acquired from National Bureau of Soil Survey and Land Use Planning (NBSS & LUP) of India. The soils were classified into B and C classes of Hydrological Soil Group (HSG). Land use data for three periods (1989, 1999 and 2009) was prepared from Landsat TM and ETM^+ imagery using supervised classification technique (Figure 2). The accuracy of classified LULC maps enhanced through post classification process by incorporating Google Earth image and local information collected during field survey.

Meteorological data is one of the most crucial input parameter in hydrological model. But, lack of climatic data in mountainous regions restricts the application of hydrological models (Marks et al., 1992). Due to unavailability of observed weather data, National Centers for Environmental Prediction (NCEP)/National Center for Atmospheric Research (NCAR) Global Reanalysis Products of Global Meteorological Forcing Dataset for Land Surface Modelling (ds314) of 1^o spatial resolution were acquired (http://rda.ucar.edu/datasets/ds314.0/) for the period 1980–2008. The daily meteorological datasets include minimum and maximum temperature, precipitation, solar radiation, wind speed and relative humidity. The database of each climate forcing file was prepared as guided in SWAT2009 input/output file documentation (Arnold et al., 2011).

The MODIS actual evapotranspiration data product (MOD16A2) prepared by Mu et al. (2007) was used for model calibration and validation. The 8-day composite actual evapotranspiration (ET_a) data of MOD16A2 product was developed at 1-km spatial resolution for the whole world based on the Penman-Monteith equation. It was prepared by combining MODIS land cover, albedo, LAI data and daily meteorological reanalysis data of 1.00°×1.25° resolution from Global Modeling and Assimilation Office (GMAO). It accounts evaporation from wet and moist soil, from rainwater intercepted by the canopy, and transpiration through stomata on plant leaves and stems occurring during both daytime and nighttime (for details see Mu et al., 2007, 2011). This data was acquired (ftp://ftp.ntsg.umt.edu/pub/MODIS/NTSG_Products/MOD16/) for the period 2004-2008. The MODIS ET_a data was considered as actual reference for calibration and validation of SWAT model.

II.3. Methods

II.3.1. SWAT model descriptions

Soil and Water Assessment Tool (SWAT) was applied for hydrological modelling via ArcGIS extension- ArcSWAT 2009 (Neitsch et al., 2011). SWAT is a basin scale, physically based semi-distributed hydrological model (Arnold et al., 1998) that is designed to simulate the effects of land management on the hydrological processes for long periods of time (Githui et al., 2009; Baker and Miller, 2013; Babar and Ramesh, 2015). The model accounts for the large-scale spatial variability of hydrological components by dividing a basin into numerous sub-basins that are further segregated into several unique hydrological response units (HRUs) based on thresholds of land use, soil types and slope classes. SWAT simulates hydrological components on a daily time step for each HRU, and routed through the channel network at the basin outlet. The minimum input data required for SWAT model setup are: (i) topographic data (DEM); (ii) soil data; (iii) LULC data; and (iv) daily meteorological data of rainfall, and minimum and maximum temperature. Based on water balance equation, SWAT calculates hydrological components include ET (potential and actual), surface runoff, lateral flow, baseflow, percolation, transmission loss etc. (Arnold et al., 1998). The detailed theoretical explanation of SWAT can be found Arnold et al (2011).

II.3.2. Model calibration and validation

Drainage network and sub-basins of Sirsa river were delineated from DEM considering a threshold of 2000 ha as minimum drainage area and fifth order stream as minimum drainage order. Reclassifying slope into four classes i.e. 0-5%, 5-15%, 15-30% and >30% (Figure 2), and overlaying with LULC and soil layers, 168, 173 and 179 numbers of HRUs were derived for 1989, 1999 and 2009 LULC, respectively. In this study, modified SCS curve number method was used for runoff estimation, Penman-Monteith method for ET estimation, and Muskingum method for channel routing. Latin Hypercube One-factor-At-a-Time (LH-OAT) based sensitivity analysis was performed to eliminate redundant parameters for calibration. Changes in model output with the variation of individual parameter values within the range given in Table 1 were experimented to enhance efficiency of calibration process.

Table 1. Description, range and optimal value of SWAT sensitive parameters that used in model calibration and validation for Sirsa basin.

Parameters	Description	Range	Optimal value
GWQMN	Threshold depth of water in the shallow aquifer required for return flow to occur (mm)	0–5000	46.44
ALPHA_BF	Base flow alpha factor (days)	0–1	0.2
REVAPMN	Threshold depth of water in the shallow aquifer for 'revap' or percolation to occur (mm)	0-500	46.5
GW_REVAP	Groundwater 'revap' coefficient	0.02–0.2	0.03
RCHR_DP	Groundwater recharge to deep aquifer (fraction)	0–1	0.36
CN2	SCS runoff CN for moisture condition II	35–98	*
CANMX	Maximum canopy storage (mm)	0–10	5
EPCO	Plant evaporation compensation factor	0.01–1	0.6
SOL_AWC	Available water capacity of the soil layer (mm H_2O/mm soil)	0–1	0.09
SOL_Z	Soil depth (mm)	0–3000	480
SOL_K	Saturated hydraulic conductivity of soil (mm/hrs)	0–100	10
ESCO	Soil evaporation compensation factor	0.01–1	0.3
GW_DELAY	Groundwater delay (days)	0–50	18

** Varies with LULC and soil types*

The simulation setup pertaining to LULC of 2009 was used to calibrate ETa for the period 2004–2006 and validate for the period 2007–2008 with MODIS ETa on monthly and daily (8-day composite) time step. The SWAT parameters were manually calibrated by editing sensitive parameters to adjust hydrological components viz. surface runoff, lateral flow, baseflow, ETa and percolation. The simulated ETa was adjusted by editing EPCO (plant evaporation compensation factor), ESCO (soil evaporation compensation factor), CANMX (maximum canopy storage), SOL_Z (soil depth), and SOL_AWC (available water capacity of the soil layer). The surface runoff was adjusted by changing CN2 (SCS curve number for moisture condition II). Re-evaporation, baseflow and deep aquifer recharge were adjusted by varying GW_REVAP (groundwater revap coefficient), REVAPMN (threshold water level in shallow aquifer for revap), GWQMN (threshold depth of water in the shallow aquifer required for return flow) and RCHR_DP (groundwater recharge to deep aquifer). Soil parameters like SOL_K (saturated hydraulic conductivity of soil) and SOL_AWC were adjusted to control lateral flow.

Initially, calibration for ETa was done for annual time step, followed by monthly and daily (8-day) time step. After closely matching SWAT simulated annual ETa with MODIS ET, parameters were fine-tuned in iterations for monthly and daily (8-day) values until the simulated results were acceptable according to performance ratings proposed by Moriasi et al. (2007). But, as the model was parameterized by comparing ETa rather than streamflow, simulation results were repeatedly checked with SWAT Check program (Arnold et al., 2012) to fine tune streamflow components. The model parameters were optimized based on statistical parameters such as coefficient of determination (R2), Nash-Sutcliffe efficiency (ENS), percent bias (PBIAS) and root mean square error-observations standard deviation ratio (RSR). The details of selected statistical parameters are given in Table 2.

Table 2. Statistics of objective functions showing the accuracy of the model during calibration (2004–2006) and validation (2007–2008).

Name	Formula	Time Step	Performance	
			Calibration	validation
Coefficient of determination	$R^2 = \left[\frac{\sum_{i=1}^{n}(O_i - \bar{O})(S_i - \bar{S})}{\sqrt{\sum_{i=1}^{n}(O_i - \bar{O})^2}\sqrt{\sum_{i=1}^{n}(S_i - \bar{S})^2}}\right]^2$	Daily	0.75	0.75
		Monthly	0.81	0.89
Nash-Sutcliffe efficiency	$E_{NS} = \left[1 - \frac{\sum_{i=1}^{n}(O_i - S_i)^2}{\sum_{i=1}^{n}(O_i - \bar{O})^2}\right]$	Daily	0.67	0.72
		Monthly	0.76	0.89
Percent bias	$PBIAS = \frac{\sum_{i=1}^{n}(O_i - S_i) * 100}{\sum_{i=1}^{n} O_i}$	Daily	2.84	2.43
		Monthly	2.84	2.43
Standardized RMSE	$RSR = \left[\frac{\sqrt{\sum_{i=1}^{n}(O_i - S_i)^2}}{\sqrt{\sum_{i=1}^{n}(O_i - \bar{O})^2}}\right]$	Daily	0.57	0.53
		Monthly	0.48	0.33

Note: *O_i: observed data of i^th^ day, $\bar{O}$: mean of observed data for the period being evaluated, S_i: simulated value of i^th^ day and $\bar{S}$: mean of simulated value for the period being evaluated.*

II.3.3. Individual impact of LULC change and climate variability

The influences of LULC change and climate variability were assessed individually by 'fixing-changing' method (Wang et al., 2009; Yan et al., 2013). In terms of the effect of LULC change alone, the simulation setups of three decadal LULCs (i.e., 1989, 1999 and 2009) were run for the constant climate period (1983–2008). For assessing climate variability impact alone, the simulation setup of 1989 LULC was run for three climate sub-periods i.e. 1983–1992, 1993–2002 and 2003–2008. The whole period (1983–2008) was sliced into three segments by the change points in trend of annual rainfall. The two change points are the lowest rainfall points corresponding to 1992 and 2002 on the 3-year moving average curve. The average annual, seasonal and monthly changes in hydrological components due to LULC change and climate variability were analyzed from SWAT output at basin and sub-basin level.

A non-parametric Mann-Kendall (MK) test including Sen's estimator of slope was applied in this study, as it was found suitable for trend analysis of hydro-meteorological data (Partal and Kahya, 2006; Li et al., 2009). The MK statistics (Zc) is calculated using following formula, where S is test statistic and sample size n>10:

$$Z_c = \begin{pmatrix} \frac{S-1}{\sqrt{Var(S)}} & if\, S > 0 \\ 0 & if\, S = 0 \\ \frac{S+1}{\sqrt{Var(S)}} & if\, S < 0 \end{pmatrix}$$

The true slope in trend was computed by the non-parametric Sen's slope (β) approach using following equation,

$$\beta = \text{median}\frac{x_j - x_k}{j-k} \quad \text{for } i = 1, \ldots, n$$

where, xj and xk are successive values at time j and k (j>k); n is the number of data, 1 <i<j<n.

II.3.4. Combined impact of LULC change and climate variability

Among the sub-periods, combined impact of LULC change and climate variability, and their separate contribution to changes in major hydrological components were analyzed through comparison of experimental runs that used alter combinations of LULC or climate. For instance, from 1983–1992 to 1993–2002 the combined impact was estimated by comparing actual scenario of two sub-periods (1989 LULC & 1983–1992 climate ~ 1999 LULC & 1993–2002 climate). The contribution of LULC change was estimated by comparing simulation from two periods LULCs for final sub-period (1989 LULC & 1993–2002 climate ~ 1999 LULC & 1993–2002 climate). Similarly, contribution of climate variability was estimated by comparing simulations that used climate data of two sub-periods and initial LULC (1989 LULC & 1983–1992 climate ~ 1989 LULC & 1993–2002 climate).

III. RESULTS AND DISCUSSIONS

III.1. SWAT model calibration and validation

The results of LH-OAT based sensitivity analysis showed that 13 parameters of SWAT model were sensitive for Sirsa basin. The model was parameterized through calibration for the period 2004–2006, and validated for the period 2007–2008 by comparing SWAT simulated ETa (Penman-Monteith) with MODIS ETa. Figure 3 represents the comparison between modelled ETa run for optimal parameters value (Table 1) and MODIS ETa at monthly and 8-day interval. The deviation of simulated ETa from MODIS ETa is very less in post-monsoon and winter seasons (October to February). The deviation varies with an average value of 2.00 mm 8-day-1 and 6.76 mm month-1. The deviation of simulated ETa increased from summer to monsoon (wet) period. During monsoon period (June to September), the deviation maximally goes up to ~18 mm 8-day-1 and ~36 mm month-1 for daily (8-day) and monthly comparison.

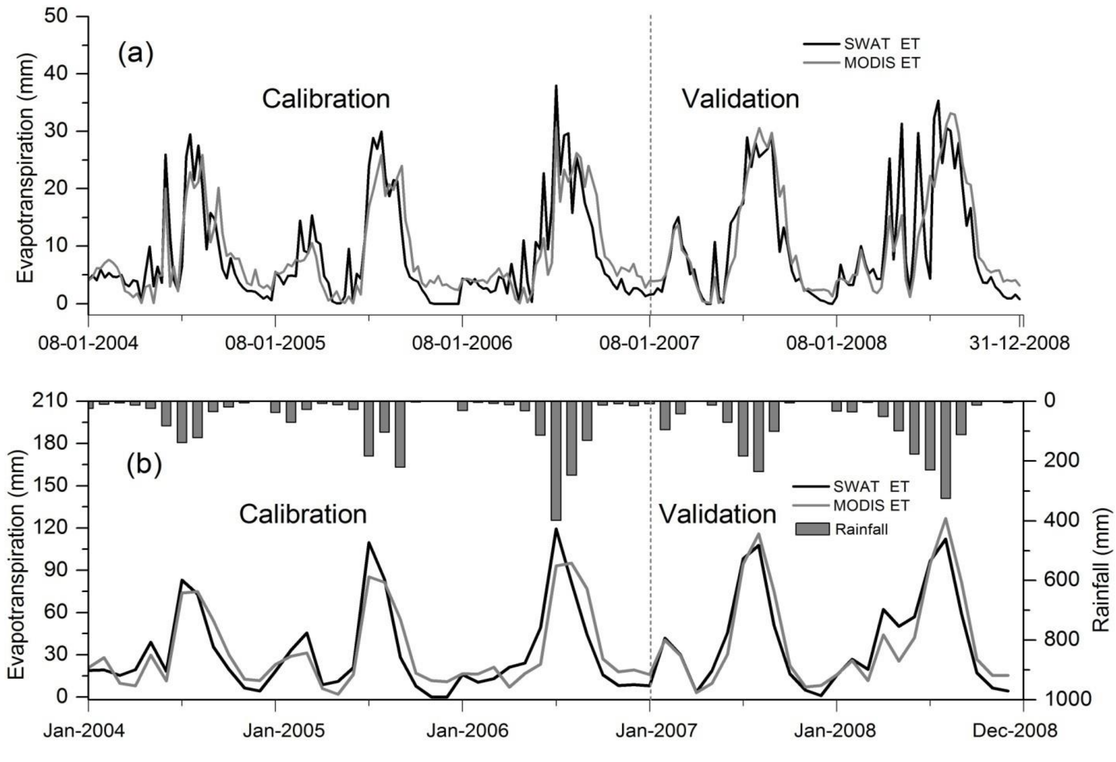

Fig. 3 Comparison between SWAT simulated ET_a and MODIS ET_a at (a) daily (8-day composite) and (b) monthly time interval during calibration period (2004–2006) and validation period (2007–2008).

The objective functions of daily (8-day) and monthly simulated ETa showed good performance of the model (Table 2). In daily (8-day) comparison, value of R2, ENS, PBIAS and RSR are 0.75, 0.67, 2.84 and 0.57, respectively, for calibration; and 0.75, 0.72, 2.43 and 0.53, respectively, for validation. Respective statistics of R2, ENS, PBIAS and RSR for monthly simulation was 0.81, 0.76, 2.84 and 0.48, respectively, in calibration; and 0.89, 0.89, 2.43 and 0.33, respectively, in validation (Table 2). The overall performance of SWAT model was 'good' for daily (8-day) simulation and 'very good' for monthly simulation according to the criteria given by Moriasi et al. (2007) for streamflow prediction.

III.2. Individual impact of LULC change and climate variability

III.2.1. Impact of LULC change

After calibration, the model was run for three LULC scenarios (1989, 1999 and 2009) for the climatic period 1983–2008. The changes in hydrological components (annual and seasonal) for the LULCs of 1999 and 2009 from the baseline LULC of 1989 is presented in Table 3. Compared to the baseline LULC of 1989, average annual streamflow (WYLD) in 1999 increased by 7.25% (24.37 mm), though average surface runoff (SURQ) decreased by 0.1% (0.22 mm). This increase in WYLD is attributed to increase in average baseflow (GWQ) and lateral flow (LATQ) by 35.61% (24.21 mm) and 0.87% (0.38 mm), respectively. But for the LULC of 2009, the average annual WYLD and SURQ increased significantly; and ETa and LATQ decreased as compared to LULC of 1989 and 1999 (Table 3).

Table 3. Change in average annual value of hydrological components (%) during dry and wet periods compared from LULC condition of 1989 to LULC of 1999 and 2009 in Sirsa basin (LULC change effect only). Seasonal change calculated as a percent of average total annual value.

Hydrological components	1989 - 1999			1989 - 2009		
	Annual	Dry	Wet	Annual	Dry	Wet
Surface runoff	-0.10	0.20	-0.30	12.12	1.91	10.21
Lateral flow	0.88	0.01	0.87	-6.69	-3.02	-3.67
Baseflow	35.62	6.22	29.40	23.57	4.20	19.37
Streamflow	7.25	1.39	5.86	12.00	1.73	10.27
ET_a	-0.67	-0.16	-0.52	-3.01	-2.07	-0.94

From 1989 to 1999, the average annual WYLD increased by 5.9% in wet season that primarily attributed to increase in GWQ (about 30%). SURQ for LULC of 2009 increased in all months over 1989, especially during monsoon period (3.0~8.2 mm month-1). Between this period, the average annual LATQ decreased by 6.7 % more or less equally in wet and dry seasons, though the relative change in dry period is high (14.5%). The simulation shows that in the last 20 years (1989 to 2009) the average annual WYLD increased by 12%, maximally in wet season (10.27%), due to LULC change. Noticeably, during the wet period, the average WYLD increased by 19.68 mm (1.1~7.7 mm month-1) for the LULC of 1999, while it increased by 34.51 mm (3.95~12.08 mm month-1) for 2009 as compared to baseline LULC.

At basin scale, changes in individual land use types and corresponding contribution to change in streamflow components in 1999 and 2009 from the baseline (1989) are presented in Table 4. From 1989 to 1999, though an increase in agricultural land (2.2%) and built-up area (1.21%) contributed to corresponding increase in average annual SURQ by 2.61% and 3.41%, respectively, in totality SURQ marginally decreased due to reduction in area under barren land (5.17). While in 2009, SURQ increased annually due to increase in contribution from cropland (12.97%) and built-up area (17.21%). From 1989 to 1999, the increase in dense forest cover has contributed to increase in average annual WYLD by 5.44%, mostly by increasing baseflow (18.05%). Though, mixed forest cover decreased by 2.87% in 1999, the result showed 6.78% hike in corresponding GWQ contribution. Similarly, in 2009, though dense and mixed forest cover decreased, the contribution of return flow increased from baseline. Apparently, it seems an error in hydrologic simulation. Clarification for this will be given in discussion section III.4.2.1.

Table 4. Basinal changes in each LULC types and corresponding change in surface runoff (SURQ), baseflow (GWQ) and streamflow (WYLD) in 1999 and 2009 from baseline LULC of 1989.

LULC types	LULC change (% of basin area)		Change in SURQ (%)		Change in GWQ (%)		Change in WYLD (%)	
	1989-1999	1989-2009	1989-1999	1989-2009	1989-1999	1989-2009	1989-1999	1989-2009
FRSE	3.16	-4.38	1.63	-2.26	18.05	6.12	5.44	-1.91
FRST	-2.87	-4.46	-2.56	-4.22	6.78	3.13	-0.98	-2.69
AGRC	2.2	9.84	2.61	12.97	9.75	17.20	3.92	13.35
BARR	-3.54	-7.67	-5.17	-11.57	1.04	-2.88	-3.41	-8.25
BU	1.21	6.54	3.41	17.21	-0.01	0.01	2.28	11.50

FRSE-Dense forest, FRST-Mixed forest, AGRC-Agricultural land, BARR-Barren land, BU-Built-up area

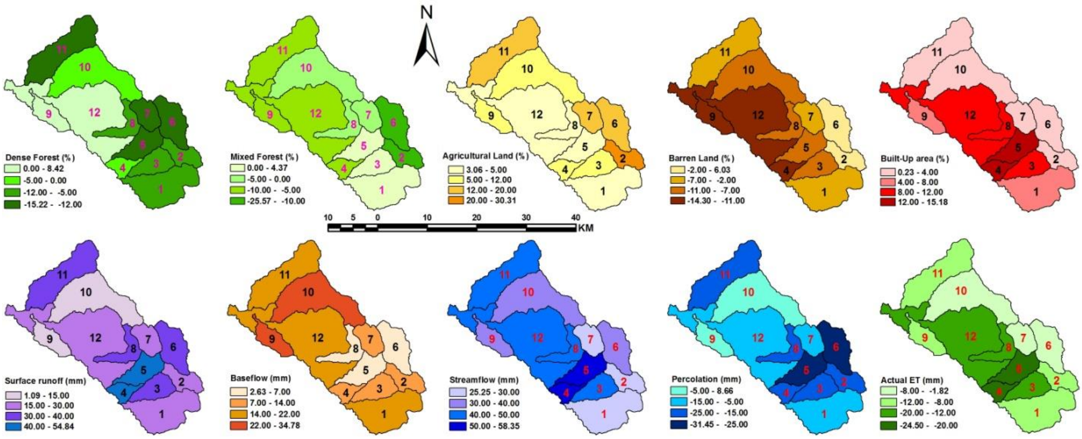

Fig. 4 Spatial distribution of changes in five LULC classes and changes in average annual hydrological components from 1989 to 2009 simulated for the climate period 1983–2008. The numbers in the map indicate corresponding sub-basin ID (#).

The spatial distribution of changes in five LULC types from 1989 and 2009 and their corresponding change in selected five hydrological components are illustrated in Figure 4. The changes in runoff closely follow the pattern of change in built-up area and dense forest cover. For example, maximum increase in SURQ and WYLD (>40 mm yr-1) is noticed in sub-basins #4 and #5, where urban expansion is maximum by more than 12% of sub-basin area. Moderate to high increase in mean annual WYLD (30–40 mm) in sub-basins #3 and #8 is associated with moderate to high expansion (8–12%) in built-up area. On the other hand, in sub-basin #6, major conversion of dense and mixed forest cover to agricultural land has attributed to significant decrease in percolation that results an increase in SURQ.

III.2.2. Impact of climate variability

Mann-Kendall test statistics (Zc) and Sen's slope (β) were applied to examine the variability in annual and monthly rainfall and temperature. During the study period (1983–2008), both, annual and monthly rainfall showed a decreasing trend, but statistically insignificant except the month of July ($p<0.05$). The average annual temperature of the basin showed significant increasing trend ($p<0.01$). The trend of average monthly temperature is increasing for all months, but statistically significant for April, July, August and October ($p<0.01$).

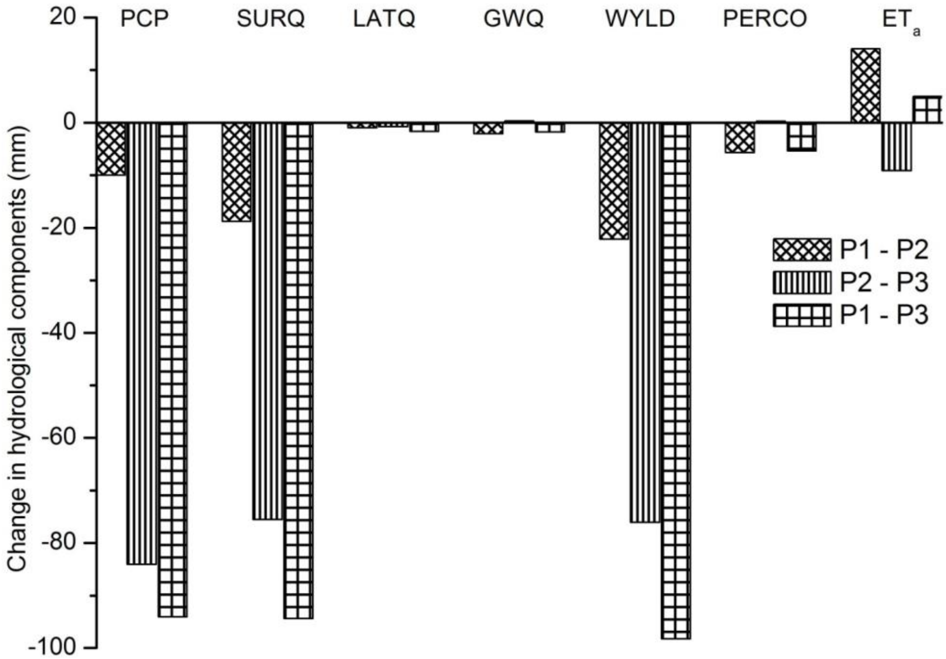

Fig. 5 Changes in average annual hydrological components in between three time periods, i.e. P1 (1983–1992), P2 (1993–2002), and P3 (2003–2008) under the impact of climate variability alone (note: PCP- rainfall, SURQ- surface runoff, LATQ- lateral flow, GWQ- baseflow, WYLD-streamflow, PERCO- percolation, ET_a- actual evapotranspiration).

The effect of climate variability on basin hydrology was separately estimated for three time-slices 1983–1992 (P1), 1993–2002 (P2) and 2003–2008 (P3) using LULC of 1989. It is noteworthy that the effects of climate variability were not found sensitive to LULCs. The average annual streamflow components have decreased in P2 and P3 from P1 as a consequence of reduction in annual rainfall (Figure 5). The annual and seasonal changes in major hydrological components between the periods are listed in Table 5. From P1 to P2, rainfall and streamflow components are marginally decreased. During dry period, the reduction in precipitation leads to decrease in LATQ and GWQ, and consequently WYLD. Noticeably, during wet period, though average annual rainfall has increased by 3.32%, the average annual SURQ and WYLD decreased by 6.0% and 3.32%, respectively. Decrease in pre-monsoon and peak monsoonal (July) rainfall is responsible for low soil moisture condition that, in turn, increases infiltration by reducing overland flow in wet period. Hence, though rainfall in rest of the wet period is increased, average SURQ decreased. This could be verified from increase of LATQ and GWQ in wet period and decrease in dry period (Table 5).

Table 5. Change in average annual hydrological components (%) in Sirsa basin in between three sub-periods (P1, P2 and P3) during dry and wet periods (climate variability effect only). Seasonal change calculated as percent of average total annual value.

Components	P1 to P2 (%)			P2 to P3 (%)			P1 to P3 (%)		
	Annual	Dry	Wet	Annual	Dry	Wet	Annual	Dry	Wet
Rainfall	-1.12	-4.44	3.32	-9.66	2.88	-12.54	-10.67	-1.59	-9.08
Surface Runoff	-7.51	-1.51	-6.00	-32.22	3.74	-35.96	-37.23	2.05	-39.28
Lateral flow	-2.22	-5.88	3.66	-1.70	1.35	-3.05	-3.88	-4.55	0.67
Baseflow	-3.42	-5.46	2.04	0.37	-1.03	1.40	-3.06	-6.46	3.40
Streamflow	-6.04	-2.72	-3.32	-22.10	2.52	-24.62	-26.80	-0.35	-26.45
Evapotranspiration	3.40	-4.85	8.25	-2.13	-1.38	-0.75	1.21	-6.27	7.47

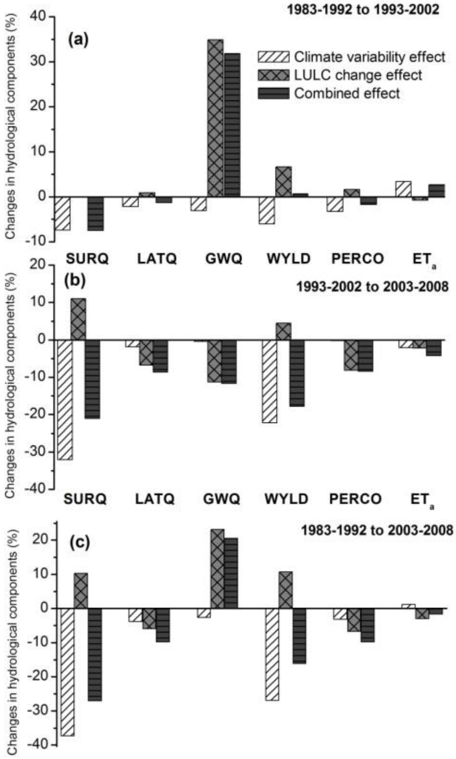

Fig. 6 Change in average annual hydrological components between three time periods: (a) 1983–1992 to 1993–2002, (b) 1993–2002 to 2003–2008, and (c) 1983–1992 to 2003–2008 under the individual and combined impact of LULC change and climate variability (note: PCP- rainfall, SURQ- surface runoff, LATQ- lateral flow, GWQ- baseflow, WYLD-streamflow, PERCO- percolation, ET$_a$- actual evapotranspiration).

As compared to P1 and P2, the amount of reduction in average annual rainfall and streamflow in P3 is quite higher (Table 5 and Figure 5). SURQ decreased in P3 by 37.23% (94.4 mm) and 32.22% (75.6 mm) from P1 and P2, respectively. Decrease in average annual runoff is attributed to decline in monsoon rainfall (wet period). Noticeably, from P1 to P3, though rainfall in dry period minimally decreased, LATQ and GWQ maximally decreased. The clarification will be made in discussion section III.4.2.2.

Compared to P1, the average annual ETa increased in P2 and P3, though it decreased and increased in dry and wet periods, respectively. From P1 to P2, change in ETa might be attributed to decrease and increase in rainfall in dry and wet periods, respectively, though the rate of increase (ETa) in wet period is high. Contrarily, from P1 to P3, average annual ETa increased in wet period by 7.47% though rainfall decreased by 9.08% (Table 5). It might be expected that complex interactions of rainfall and temperature brings changes in average annual ETa.

III.3.Combined impact of LULC change and climate variability

LULC change and climate variability together have caused a phenomenal decrease in average annual value of most of hydrological components between the time-slices from 1983 to 2008 (Figure 6). The combined and relative impact of LULC change and climate variability on WYLD is provided in Table 6. Between the three time-slices, LULC change and climate variability separately impacted positive and negative influence, respectively, on average annual SURQ and WYLD. When the influence of climate variability was found stronger than LULC change, average annual WYLD is decreased. For example, from P1 to P3, the average annual WYLD reduced by 16.1% (58.86 mm) as climate variability (mainly rainfall) alone impacted to decline by 26.8% (98.24 mm), albeit, changes in LULC (1989 to 2009) boosted to increase the flow by 10.7% (39.38 mm) increase.

Table 6. Combined and relative impact of LULC change and climate variability on average annual streamflow between three periods (combined impact).

Streamflow (mm) in periods		Change (mm)	Relative change	Remarks
1983-1992	1993-2002			
365.83 (LU1)	368.07 (LU2)	2.24	---	Combined effect
	343.68 (LU1)	24.39	+52.41%	LUCC effect
		-22.15	-47.59%	Climate variability
1993-2002	2003-2008			

368.07 (LU2)	306.97 (LU3)	-61.1	----	Combined effect
	291.66 (LU2)	15.31	+16.69%	LUCC effect
		-76.41	-83.31%	Climate variability
1983-1992	2003-2008			
365.83 (LU1)	306.97 (LU3)	-58.86	---	Combined effect
	267.59 (LU1)	39.38	28.62%	LUCC effect
		-98.24	-71.38%	Climate variability

Note: LU1, LU2 and LU3 denote simulations using LULC of 1989, 1999 and 2009, respectively.

The average annual GWQ of the basin increased in P2 and P3 as compared to P1 by 31.8% and 20.5%, respectively, as a result of LULC change. In the case of LATQ and percolation, though LULC change and climate variability controlled in same direction to decrease the average annual value, the impact of LULC change is dominant (Figure 6). As compared to P1 and P2, the average annual ETa of the basin decreased in P3 (<5%), mostly due to the negative impact of LULC change. Interestingly, though average annual rainfall decreased in P2 and P3 as compared to P1, climate variability alone tended to increase average annual ETa. This might be caused due to increase in air temperature.

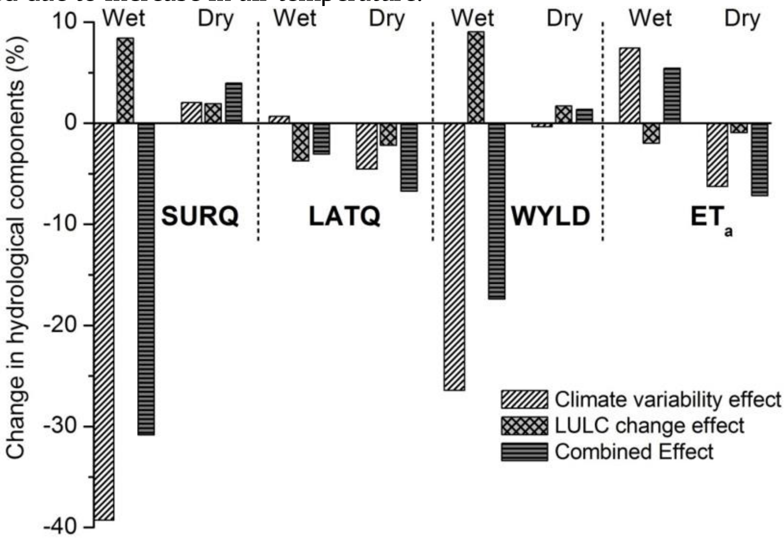

Fig. 7 Change in average annual hydrological components in wet and dry periods under the individual and combined impact of LULC change and climate variability from P1 (1983–1992) to P3 (2003–2008). Here, SURQ- surface runoff, LATQ- lateral flow, WYLD-streamflow, ET_a- actual evapotranspiration.

The combined impact of LULC change and climate variability on seasonal changes of SURQ, LATQ, WYLD and ETa (P1~P3) is presented in Figure 7. The combined impact on SURQ and WYLD during wet period is closely following same pattern of climate variability impact as shown in Figure 6. During this period, though the average annual rainfall decreased in dry period by 1.6% (14 mm), average annual SURQ increased by 2% (5.2 mm) (Table 5). This is because of increase in average rainfall in February by 12.9 mm that tended to increase in runoff by 7.7 mm. Overall, LATQ decreased in dry and wet period, though maximally in dry period (6.7%) as climate variability and LULC change impacted in the same direction to decrease its value. The influence of climate variability on seasonal change of average annual ETa is stronger than the impact of LULC change. From the combined effect, the average annual ETa decreased by 7.1% in dry period, and increased by 5.5% in wet period, of which climate variability alone accounts 6.6% and 7.5% to decrease and increase in respective periods.

III.4. Discussion

III.4.1 SWAT model calibration and validation

In this study, considering MODIS ETa data (MOD16A2) as ground observation, SWAT model was parameterized by comparing simulated ETa. The model overestimated ETa during pre-monsoon and monsoon period, especially April–July; and underestimated in post monsoon and winter season. The result showed that during peak rainfall period (July), the median of difference of simulation from MODIS ETa is less than 10 mm month-1. The objective functions (Table 2) reflect that the performance of the model during validation period is quite better than calibration in both, daily (8-day) and monthly comparisons. This is because higher overestimation of the model in calibration period than validation period during wet season.

On the other hand, the difference in climate data that has been used for SWAT simulation and MODIS ETa estimation may be responsible for such variations. For instance, the noticeable difference between SWAT ETa and MODIS ETa in the month of April–May in 2008 (Figure 3) is expected as the outcome of difference in rainfall data between NCEP (used in SWAT) and GMAO (used for MODIS ETa). By comparing the whole period (1983–2008), an excessive high rainfall in these months has been found for NCEP data in 2008. However, high uncertainty of daily gridded rainfall data (Chappell et al., 2013) and error within remote sensing data (Jarihani et al., 2015) can increase uncertainty in model prediction.

For the simulation of ETa, calibration of hydrological model using satellite-based ETa may give better performance than by using observed streamflow data (Rientjes et al., 2013). But for assessment of streamflow components, parameterization of distributed hydrological model with ETa data can produce ambiguity in separation of streamflow components. Rientjes et al. (2013) found that low simulation of baseflow accounts poor performance for streamflow estimation while only satellite-based ETa used for model calibration. This is due to the fact that the parameters that control ET simulation may exert limited influence on streamflow components and groundwater recharge. To minimize the error in streamflow simulation, the model parameters were adjusted by repeatedly checking SWAT outputs with SWAT Check program (Arnold et al., 2012). Uncertainty in SWAT simulation in this calibration approach could be better understood if it is further applied for a gauge basin. However, overall good statistical performance indicates that the calibrated SWAT model could be effectively applied for simulation of other hydrological components.

III.4.2. Individual impact of LULC change and climate variability

III.4.2.1 Impact of LULC change

Average annual WYLD substantially increased in 1999 when compared with baseline LULC (1989), though average annual SURQ marginally decreased. This is attributed to increase in baseflow through increasing interception and infiltration as dense forest cover increased over mixed forest and barren land. This suggests that LULC change controls WYLD by modifying the partition of rainfall into overland flow and infiltration processes (Juckem et al., 2008). The invasion of built-up area and agricultural land over forest cover in 2009, as compared to 1989 and 1999, has lead to noticeable increase in SURQ by increasing the conversion of precipitation into overland flow, rather than sub-surface flow and percolation (Mustard and Fisher, 2004; Shanahan and Jacobs, 2007; Nie et al., 2011). The increase in runoff is mostly attributed in wet season because of increase in peak discharge during monsoon season that attributed to urbanization and deforestation (Zhou et al., 2013; Miller et al., 2014). The analysis suggests that SURQ will increase simultaneously with time while land use modification with urbanization continues in the future.

Increase of GWQ in 1999 over 1989 is dominantly attributed to increase of dense forest cover. Increase in canopy cover induced the contribution of return flow to streamflow through increasing infiltration capacity (Ma et al., 2009). From 1989 to 2009, increase in GWQ is majorly attributed to increase in agricultural land (Juckem et al., 2008), though forest cover decreased. Interestingly, though average annual percolation decreased by 11.9 mm from 1989 to 2009, GWQ increased. This could be due to replacement of forest cover and barren land by agricultural land. Increase in GWQ apparently outweighs the reduction in ETa (12.5 mm yr-1) due to decrease in interception and water usage on account of reduction in forest cover (Paco et al., 2009; Price, 2011). However, previous studies showed that the baseflow could increase or decrease with deforestation depending on complex balance between infiltration and ETa (see Price, 2011).

At basin scale, the actual contribution of mixed forest to GWQ increased in 1999 and 2009, though its area decreased compared to 1989 (Table 4). This contradiction at basin scale has been resulted from inter sub-basinal variation in forest cover change and corresponding contribution to GWQ rather than simulation error. For example, in 1999, the maximum increase of GWQ under mixed forest in the basin is corresponding to sub-basin #9 that experienced increase in mixed forest cover. Similarly, in 2009, major increase in GWQ contribution from dense forest is noticed for sub-basins #9 and #12; and major increase in contribution from mixed forest is noticed in sub-basins #1, #3 and #5. Though forest cover in these sub-basins increased, corresponding area cumulatively decreased at basin scale. Hence, it is suggested that understanding of complex relation between change in each LULC type and corresponding hydrologic response among sub-basins might clearly reflect the impact of LULC change at basin scale. Moreover, as topography plays an important role in percolation, change in GWQ may not linearly correlate with forest cover change in a heterogeneous basin.

The change in ETa is more or less similarly correlated with all LULC types. But, the pattern of decrease in average annual ETa is closely matched with increase in the built-up area (Figure 4). As built-up area increases, canopy cover is removed, which minimizes transpiration process from plants and evaporation from soil. These findings agree with previous studies in China (Nie et al., 2011; Zhou et al., 2013).

III.4.2.2. Impact of climate variability

As compared to the effect of LULC change alone, climate variability was found superior to control hydrological processes in Sirsa basin. Climate variability alone has substantially decreased SURQ and WYLD in P3 (2003–2008) as compared to P1 (1983–1992) and P2 (1993–2002) due to decrease in rainfall by about 10%, though the trend is statistically insignificant. Additionally, decrease in rainfall in wet months reduced LATQ and GWQ in dry period, especially post-monsoon period, though it increased nominally wet season. The time lag between rainfall events and its conversion to LATQ and GWQ has caused such variation. For example, from P1 to P3, average annual GWQ maximally decreased in October by 5.57% as average annual rainfall decreased by 10.5% in July–September.

From P to P2 and P3, the decrease and increase of ETa in dry and wet season, respectively, is governed by the change in rainfall and temperature in a complex way. Since average monthly temperature in wet season significantly increased, the evaporation rate enhanced (Trenberth, 1999; Tan et al., 2015) despite decrease in precipitation (Jha and Gassman, 2014). The decrease in infiltration as a consequence of decrease in monsoonal rainfall has failed to meet plant root uptake sufficiently in dry season. This might be responsible for decrease in ETa in dry period. However, the estimated impacts of climate variability are more pronounced for the seasonal variability in ETa than the annual variability.

III.4.3. Combined impact of LULC change and climate variability

The impacts of LULC change alone and climate variability alone on SURQ and WYLD were almost opposite in direction, resulting in a reduction of total impact (Khoi and Suetsugi, 2014). When compared to the reference period P1 (1983–1992), there was only a marginal increase in average annual WYLD for P2 (1993–2002) because the impact of LULC change (increase in WYLD) was offset by climate variability (decrease in WYLD). But between these periods, change in SURQ from combined effect is consistent to that under climate variability alone while LULC change showed negligible sensitivity. During P3 (2003–2008), the average annual SURQ of the basin decreased as compared to P1 and P2 because the impact of climate variability is too dominant to reduce runoff than the impact of LULC change to increase runoff. From P1 to P3, average annual SURQ and WYLD significantly declined in the wet season and increased in dry season under the combined impact of LULC change and climate variability. During the dry period, WYLD is dominantly controlled by LULC change, though SURQ controlled by LULC change and climate variability in the same direction and same magnitude (Figure 7). However, in consistence with some previous studies (Ma et al., 2010; Tang et al., 2011; Bao et al., 2012), in this study climate variability was found as the major driving factor for controlling WYLD rather than LULC change.

In this study GWQ is found most sensitive to LULC change than climate variability. Between three time-slices, the scenario of change in average annual GWQ from combined impact is similar to that under LULC change alone (Figure 6). As compared from P1 and P2 to P3, the decrease in LATQ and percolation is triggered under the combined impact as LULC change and climate variability individually acted in a similar direction, though control of LULC change is dominant. However, in this study, LULC change exerts more control on infiltration and percolation processes than climate variability. This finding could be supported by previous study by Juckem et al. (2008) that showed significant control of land use practice and management on GWQ.

This study shows that the impact of LULC change on average annual ETa is dominant (decreasing ETa) than that of climate variability, when P3 is compared with P1 and P2. Since the impact of climate variability on seasonal changes of ETa acted in opposite direction, total impact on annual value is reduced. Therefore, while seasonal changes are compared, climate variability overrides the impact of LULC change. For example, from P1 to P3 average annual ETa increased and decreased (by >5%) in wet and dry periods respectively, from combined impact as significant consequences of climate variability. The clarification of ETa response to seasonal variations is suggested to be similar to that as it is discussed for climate variability impact alone on ETa (section 5.2.2).

III.5. Limitations

The analysis of hydrological responses employing hydrological models entail many limitations and uncertainties associated with input data, model structure, and model parameters (Lindenschmidt et al., 2007). Instead of station meteorological data, this study used NCEP/NCAR reanalysis output (1o x 1o). This dataset is too coarse to incorporate spatial variability of climate, especially rainfall. Moreover, uncertainty in reanalysis data to capture observed trends (McVicar et al., 2012) is a major limitation of this study. Though, several hydrological components were simulated through SWAT model, the model parameters were calibrated only using MODIS ETa data. Hence, predicted hydrological components contain uncertainty, especially in separation of baseflow from streamflow, and segregation of shallow and deep aquifer recharge. Concomitantly, meteorological data used in calculation of ETa for SWAT and MODIS data are different. Thus, comparison of these two ETa data contains uncertainty. Furthermore, model parameters were adjusted for only LULC scenario of 2009 without calibrating simulation setups of LULC scenario of 1989 and 1999. These uncertainty and limitations are unwillingly incorporated in this study for understanding hydrological response of ungauged river basin.

IV. CONCLUSIONS

In this study, hydrological consequences of LULC change and climate variability were evaluated for an ungauged basin in North-Western Himalaya using SWAT model that was calibrated and validated with MODIS ETa data for the period of 2004–2008. The individual and combined impacts of LULC change and climate variability on major hydrological components were analyzed annually and seasonally. LULC conversion in the basin from 1989 to 2009 led to increase in average annual surface runoff and streamflow each by about 12%. Increase in cropland (9.8%) and built-up area (6.5%) from 1989 to 2009 has individually contributed to increase in surface runoff by 13% and 17.2%, respectively. Average annual lateral flow of the basin is decreased by 6.7% (1989 to 2009) as a significant consequence of forest cover reduction. Replacement of forest cover and barren land by cropland from 1989 to 2009 was identified as the strongest contributor to increase baseflow.

Climate variability has noticeably impacted on streamflow components to decrease between sub-periods from 1983 to 2008. The average annual surface runoff is decreased by 37.30% in between 1983–1992 and 2003–2008 due to decrease in rainfall by 10.7%. Similarly, decline in monsoonal rainfall, especially in July and September, has dramatically reduced annual streamflow (>22%) in 2003–2008 as compared to 1983–1992 and 1993–2002. Besides, climate variability has impacted to reduce lateral flow and baseflow during dry periods, especially during post-monsoon periods. Since LULC change is causing runoff to increase and climate variability is causing runoff to decrease, the combined effect of the two leads to decrease annual streamflow, because role of climate variability is dominant as compared to LULC change.

Industrialization and rapid population growth in the basin, especially in Baddi-Barotiwala-Nalagarh region has dramatically altered land use of the basin in last two decade. Increase in surface runoff and decline in percolation resulted from LULC change has created a negative impact on hydrology of Sirsa river basin. The impact of LULC change on percolation is elevated by climate variability as rainfall is showing a decreasing trend. Hence, decline in percolation on the one hand, and increasing demand of water on the other hand will exacerbate water availability for future. Therefore, this study would help stakeholders and planners for sustainable management of water resources emphasizing adaptation to climate variation and LULC change. Besides, the study will also improve our knowledge of interactions of each land cover type on hydrological processes, especially for data-scarce river basins.

Acknowledgement

The first author is grateful to Council of Scientific and Industrial Research (CSIR), New Delhi for providing financial support for the present work as a doctoral fellowship. The authors are also thankful to Director, IIRS, Dehradun and Head, Dept. of Geography, BHU, Varanasi for providing research facilities. NASA- METI, USGS, CSIL and MODIS are highly acknowledged for providing freely available data used in this study. Anonymous reviewers are greatly acknowledged for their very fruitful comments and suggestions that improved the quality of our original manuscript.

References

Anav, A., Ruti, P., Artale, V., Valentini, R., 2010. Modelling the effects of land-cover changes on surface climate in the Mediterranean region. Climate Res. 41, 91-104.

Andersen, J., Dybkjaer, G., Jensen, K.H., Refsgaard, J.C., Rasmussen, K., 2002. Use of remotely sensed precipitation and leaf area index in a distributed hydrological model. J. Hydrol. 264, 34–50.

Arnold, J.G., Kiniry, J.R., Srinivasan, R., Williams, J.R., Haney, E.B., Neitsch, S.L. 2011. Soil and Water Assessment Tool Input/Output File Documentation. Version 2009.

Grassland, Soil, and Water Research Laboratory, Agriculture Research Service, Texas A&M University System.

Arnold, J.G., Moriasi, D.N., Gassman, P.W., Abbaspour, K.C., White, M.J., et al., 2012. SWAT: model use, calibration, and validation. ASABE 55 (4), 1491-1508.

Arnold, J.G., Srinivasan, R., Muttiah, R.S., Williams, J.R., 1998. Large area hydrologic modeling and assessment – Part I: Model development. JAWRA 34 (1), 73–89.

Babar, S., Ramesh, H., 2015. Streamflow Response to Land Use–Land Cover Change over the Nethravathi River Basin, India. J. Hydrol. Eng. DOI:10.1061/(ASCE)HE.1943-5584.0001177.

Baker, T.J., Miller, S.N., 2013. Using the Soil and Water Assessment Tool (SWAT) to assess land use impact on water resources in an East African watershed. J. Hydrol. 486, 100–111.

Bao, Z., Zhang, J., Wang, G., Fu, G., He, R., Yan, X., Jin, J., Liu, Y., Zhang, A., 2012. Attribution for decreasing streamflow of the Haihe River basin, northern China: climate variability or human activities? J. Hydrol. 460, 117–129.

Beck, H.E., Bruijnzeel, L.A., van Dijk, A.I.J.M., McVicar, T.R., Scatena, F.N., Schellekens, J., 2013. The impact of forest regeneration on streamflow in 12 mesoscale humid tropical catchments. Hydrol. Earth Syst. Sci. 17, 2613–2635.

Beven, K.J., Freer, J., 2001. Equifinality, data assimilation, and uncertainty estimation in mechanistic modelling of complex environmental systems. J. Hydrol. 249, 11–29.

Callow, J.N., Boggs, G.S., 2013. Studying reach-scale spatial hydrology in ungauged catchments. J. Hydrol. 496, 31–46.

Campo, L., Caparrini, F., Castelli, F., 2006, Use of multi-platform, multi-temporal remote-sensing data for calibration of a distributed hydrological model: an application in the Arno basin, Italy. Hydrol. Process. 20, 2693–2712.

Chappell, A., Renzullo, L.J., Raupach, T.H., Haylock, M., 2013. Evaluating geostatistical methods of blending satellite and gauge data to estimate near real-time daily rainfall for Australia. J. Hydrol. 493, 105–114.

Chen, J.M., Chen, X., Ju, W., Geng, X., 2005. Distributed hydrological model for mapping evapotranspiration using remote sensing inputs. J. Hydrol. 305, 15–39.

Costa, M.H., Botta, A., Cardille, J.A., 2003. Effects of large-scale changes in land cover on the discharge of the Tocantins River, Southeastern Amazonia. J. Hydrol. 283, 206–217.

Dash, P., Aggarwal, S.P., Verma, N., Ghosh, S., 2014. Investigation of scale dependence and geomorphic stages of evolution through hypsometric analysis: A case study of Sirsa basin, western Himalaya, India. Geocarto Int. 29 (7), 758-777.

Deng, X., Shi, Q., Zhang, Q., Shi, C., Yin, F., 2015. Impacts of land use and land cover changes on surface energy and water balance in the Heihe River Basin of China, 2000–2010. Phys. Chem. Earth. 79–82, 2–10.

Eckhardt, K., Ulbrich, U., 2003. Potential impacts of climate change on groundwater recharge and streamflow in a central European low mountain range. J Hydrol. 284, 244–252.

Eshtawi, T., Evers, M., Tischbein, B., 2015. Quantifying the impact of urban area expansion on groundwater recharge and surface runoff. Hydrolog. Sci. J. DOI: 10.1080/02626667.2014.1000916.

Frappart, F. et al., 2008. Interannual variations of river water storage from a multiple satellite approach: a case study for the Rio Negro River basin. J. Geophys. Res.: Atmosp. 113 (D21), D21104.

Githui, F., Gitau, W., Mutua, F., Bauwens, W., 2009. Climate change impact on SWAT simulated streamflow in western Kenya. Int. J. Climatol. 29, 1823–1834.

Githui, F., Selle, B., Thayalakumaran, T., 2012. Recharge estimation using remotely sensed evapotranspiration in an irrigated catchment in southeast Australia. Hydrol. Process. 26, 1379–1389.

Götzinger, J., Bárdossy, A., 2007. Comparison of four regionalisation methods for a distributed hydrological model. J. Hydrol. 333, 374–384.

Gu, C., Hu, L., Zhang, X., Wang, X., Guo, J., 2011. Climate change and urbanization in the Yangtze River Delta. Habitat. Int. 35, 544-552.

Guan, M., Sillanpää, N., Koivusalo, H., 2015. Storm runoff response to rainfall pattern, magnitude and urbanization in a developing urban catchment. Hydrol. Process. DOI: 10.1002/hyp.10624.

Immerzeel, W.W., Droogers, P., 2008. Calibration of a distributed hydrological model based on satellite evapotranspiration. J. Hydrol. 349, 411-424.

Jha, M.K., Gassman, P.W., 2014. Changes in hydrology and streamflow as predicted by a modelling experiment forced with climate models. Hydrol. Process. 28, 2772–2781.

Jhorar, R.K., Smit, A.A.M.F.R., Bastiaanssen, W.G.M., Roest, C.W.J., 2011. Calibration of a distributed irrigation water management model using remotely sensed evapotranspiration rates and groundwater heads. Irrig. and Drain. 60, 57–69.

Juckem, P.F., Hunt, R.J., Anderson, M.P., Robertson, D.M., 2008. Effects of climate and land management change on streamflow in the driftless area of Wisconsin. J. Hydrol. 355, 123–130.

Khoi, D.N., Suetsugi, T., 2014. Impact of climate and land-use changes on hydrological processes and sediment yield—a case study of the Be River catchment, Vietnam. Hydrolog. Sci. J. 59 (5), 1095-1108.

Lakshmi, V., 2004. The role of satellite remote sensing in the Prediction of Ungauged Basins. Hydrol. Process.18, 1029–1034.

Li, Q., Cai, T., Yu, M., Lu, G., Xie, W., Bai, X., 2013. Investigation into the Impacts of Land-Use Change on Runoff Generation Characteristics in the Upper Huaihe River Basin, China. J. Hydrol. Eng. 18, 1464-1470.

Li, Z., Liu, W.Z., Zhang, X.C., Zheng, F., 2009. Impacts of land use change and climate variability on hydrology in an agricultural catchment on the Loess Plateau of China. J. Hydrol. 377, 35–42.

Lindenschmidt, K.E., Fleischbein, K., Baborowski, M., 2007. Structural uncertainty in a river water quality modelling system, Ecol. Model., 204, 289–300.

Ma, H., Yang, D.W., Tan, S.K., Gao, B., Hu, Q.F., 2010. Impact of climate variability and human activity on streamflow decrease in Miyun Reservoir catchment. J. Hydrol. 389, 317–324.

Ma, X., Xu, J., Luo, Y., Aggarwal, S.P., Li, J., 2009. Response of hydrological processes to land-cover and climate changes in Kejie watershed, south-west China. Hydrol. Process. 23, 1179–1191.

Mango, L.M., Melesse, A.M., McClain, M.E., Gann, D., Setegn, S.G., 2011. Land use and climate change impacts on the hydrology of the upper Mara River Basin, Kenya: results of a modeling study to support better resource management. Hydrol. Earth Syst. Sci. 15, 2245–2258.

Mao, D., Cherkauer, K.A., 2009. Impacts of land-use change on hydrologic responses in the Great Lakes region, J. Hydrol. 374 (1–2), 71–82.

Marks, D., Dozier, J., Davis, R.E., 1992. Climate and energy exchange at the snow surface in the Alpine Region of the Sierra Nevada: 1. Meteorological measurements and monitoring. Water Resour. Res. 28 (11), 3029–3042.

McVicar, T.R. et al., 2012. Global review and synthesis of trends in observed terrestrial near-surface wind speeds: Implications for evaporation. J. Hydrol. 416–417, 182–205.

Miller, J.D., Kim, H., Kjeldsen, T.R., Packman, J., Grebby, S., Dearden, R., 2014. Assessing the impact of urbanization on storm runoff in a peri-urban catchment using historical change in impervious cover. J. Hydrol. 515, 59–70.

Moriasi, D.N., Arnold, J.G., Van Liew, M.W., Bingner, R.L., Harmel, R.D., Veith, T.L., 2007. Model evaluation guidelines for systematic quantification of accuracy in watershed simulations, Trans. ASABE 50, 885–900.

Mu, Q., Heinsch, F.A., Zhao, M., Running, S.W., 2007. Development of a global evapotranspiration algorithm based on MODIS and global meteorology data. Remote Sens. Environ. 111, 519−536.

Mu, Q., Zhao, M., Running, S.W., 2011. Improvements to a MODIS global terrestrial evapotranspiration algorithm. Remote Sens. Environ. 115, 1781–1800.

Mustard, J., Fisher, T., 2004. Land Use and Hydrology. In: Gutman, G., Janetos, A., Justice, C., Moran, E., Mustard, J., Rindfuss, R., Skole, D., Turner, B.L. and Cochrane, M. (Eds.), Land Change Science: Observing Monitoring and Understanding Trajectories of Change on the Earth's Surface. Kluwer Academic Publishers, Dordrecht, The Netherlands, pp. 257-276.

Neitsch, S.L., Arnold, J.G., Kiniry, J.R., Williams, J.R., 2011. Soil and water assessment tool theoretical documentation. Version 2009. Grassland, Soil, and Water Research Laboratory, Agriculture Research Service, Texas A&M University System.

Nie, W., Yuan, Y., Kepner, W., Nash, M.S., Jackson, M., Erickson, C., 2011. Assessing impacts of Landuse and Landcover changes on hydrology for the upper San Pedro watershed. J. Hydrol. 407, 105–114.

Paco, T.A., David, T.S., Henriques, M.O., Pereira, J.S., Valente, F., Banza, J., Pereira, F.L., Pinto, C., David, J.S., 2009. Evapotranspiration from a Mediterranean evergreen oak savannah: The role of trees and pasture. J. Hydrol. 369, 98–106.

Parajka, J., Merz, R., Bloschl, G., 2005. A comparison of regionalisation methods for catchment model parameters. Hydrol. Earth Syst. Sci. 9, 157–171.

Partal, T., Kahya, E., 2006. Trend analysis in Turkish precipitation data. Hydrol. Process. 20, 2011–2026.

Peña-Arancibia, J.L., van Dijk, A.I.L.J.M., Guerschman, J.P., Mulligan, M., Bruijnzeel, L.A., McVicar, T.R., 2012. Detecting changes in streamflow after partial woodland clearing in two large catchments in the seasonal tropics. J. Hydrol. 416–417, 60–71.

Price, K., 2011. Effects of watershed topography, soils, land use, and climate on baseflow hydrology in humid regions: A review. Prog. Phys. Geog. 35(4), 465–492.

Rientjes, T.H.M., Muthuwatta, L.P., Bos, M.G., Booij, M.J., Bhatti, H.A., 2013. Multi-variable calibration of a semi-distributed hydrological model using streamflow data and satellite-based evapotranspiration. J. Hydrol. 505, 276–290.

Samuel, J., Coulibaly, P., Metcalfe, R.A., 2011. Estimation of Continuous Streamflow in Ontario Ungauged Basins: Comparison of Regionalization Methods. J. Hydrol. Eng. 16 (5), 447–459.

Sanyal, J., Densmore, A.L., Carbonneau, P., 2014. Analysing the effect of land-use/cover changes at sub-catchment levels on downstreamflood peaks: A semi-distributed modelling approach with sparse data. Catena 118, 28–40.

Sellami, H., La Jeunesse, I., Benabdallah, S., Baghdadi, N. and Vanclooster, M. 2014. Uncertainty analysis in model parameters regionalization: a case study involving the SWAT model in Mediterranean catchments (Southern France). Hydrol. Earth Syst. Sci., 18, 2393–2413.

Shanahan, P., Jacobs, B.L., 2007. Ground water and cities. In: Novotny, V., Brown, P.R. (Eds.), Cities of the Future: Towards Integrated Sustainable Water and Landscape Management. IWA Publishing, London, pp. 122-140.

Stehr, A., Debels, P., Arumi, J.L., Romero, F., Alcayaga, H., 2009. Combining the Soil and Water Assessment Tool (SWAT) and MODIS imagery to estimate monthly flows in a datascarce Chilean Andean basin. Hydrolog. Sci. J. 54 (6), 1053-1067.

Tan, M.L., Ibrahim, A.L., Yusop, Z., Duan, Z., Ling, L., 2015. Impacts of land-use and climate variability on hydrological components in the Johor River basin, Malaysia. Hydrolog. Sci. J. 60 (5), 873-889.

Tang, L., Yang, D., Hu, H., Gao, B., 2011. Detecting the effect of land-use change on streamflow, sediment and nutrient losses by distributed hydrological simulation. J. Hydrol. 409, 172–182.

Tran, L.T., O'Neill, R.V., 2013. Detecting the effects of land use/land cover on mean annual streamflow in the Upper Mississippi River Basin, USA. J. Hydrol. 499, 82–90.

Trenberth, K.E., 1999. Conceptual framework for changes of extremes of the hydrological cycle with climate change. Climatic Change 42, 327–339.

Wang, G., Xia, J., Chen, J., 2009. Quantification of effects of climate variations and human activities on runoff by a monthly water balance model: A case study of the Chaobai River basin in northern China. Water Resour. Res. 45, W00A11, doi:10.1029/2007WR006768.

Wilson, C.O., Weng, Q., 2011. Simulating the impacts of future land use and climate changes on surface water quality in the Des Plaines River watershed, Chicago Metropolitan Statistical Area, Illinois. Sci. Total Environ. 409, 4387–4405.

Wu, K., Johnston, C.A., 2007. Hydrologic response to climatic variability in a Great Lakes Watershed: a case study with the SWAT model. J. Hydrol. 337, 187–199.

Yan, B., Fang, N.F., Zhang, P.C., Shi, Z.H., 2013. Impacts of land use change on watershed streamflow and sediment yield: An assessment using hydrologic modelling and partial least squares regression. J. Hydrol. 484, 26–37.

Zhang, J. et al., 2004. Estimation of river discharge using TOPEX/Poseidon altimeter data. Acta Geographica Sinica 59 (1), 95–100.

Zhang, X., Srinivasan, R., Hao, F., 2007. Predicting hydrologic response to climate change in the Luohe river basin using the SWAT model. ASABE 50 (3), 901-910.

Zhang, Y.K., Schilling, K.E., 2006. Effects of land cover on water table, soil moisture, evapotranspiration, and groundwater recharge: A Field observation and analysis. J. Hydrol. 319, 328–338.

Zhao, C., Liu, C., Dai, X., Liu, T., Duan, Z., Liu, L., Mitrovic, S.M., 2015. Separation of the impacts of climate change and human activity on runoff variations. Hydrolog. Sci. J.60 (2), 234-246.

Zhou, F., Xu, Y., Chen, Y., Xu, C.H., Gao, Y., Du, J., 2013. Hydrological Response to Urbanization at Different Spatio-temporal Scales simulated by coupling of CLUE-S and the SWAT model in the Yangtze River Delta region. J. Hydrol. 485, 113–125.

Received: 20.09.2017
Revised: 12.02.2018
Accepted: 26.11.2018
Published: 28.12.2018